



Linking the Water and Carbon Economies of Plants in a Drying and Warming Climate

Mazen Nakad¹ · Sanna Sevanto² · Jean-Christophe Domec^{3,4} · Gabriel Katul^{1,4}

Accepted: 14 September 2023 / Published online: 23 October 2023
© The Author(s), under exclusive licence to Springer Nature Switzerland AG 2023

Abstract

Purpose of Review Harsher abiotic conditions are projected for many woodland areas, especially in already arid and semi-arid climates such as the Southwestern USA. Stomatal regulation of their aperture is one of the ways plants cope with drought. Interestingly, the dominant species in the Southwest USA, like in many other ecosystems, have different stomatal behaviors to regulate water loss ranging from isohydric (e.g., piñon pine) to anisohydric (e.g., juniper) conditions suggesting a possible niche separation or different but comparable strategies of coping with stress. The relatively isohydric piñon pine is usually presumed to be more sensitive to drought or less desiccation tolerant compared to the anisohydric juniper although both species close their stomata under drought to avoid hydraulic failure, and the mortality of one species (mostly piñon) over the other in the recent droughts can be attributed to insect outbreaks rather than drought sensitivity alone. Furthermore, no clear evidence exists demonstrating that iso- or anisohydric strategy increases water use efficiency over the other consistently. How these different stomatal regulatory tactics enable woody species to withstand harsh abiotic conditions remains a subject of inquiry to be covered in this review.

Recent Findings This contribution reviews and explores the use of simplified stomatal optimization theories to assess how photosynthesis and transpiration respond to warming (H), drought (D), and combined warming and drought (H+D) for isohydric and anisohydric woody plants experiencing the same abiotic stressors. It sheds light on how simplified stomatal optimization theories can separate between photosynthetic and hydraulic acclimation due to abiotic stressors and how the interactive effects of H+D versus H or D alone can be incorporated into future climate models.

Summary The work here demonstrates how field data can be bridged to simplified optimality principles so as to explore the effect of future changes in temperature and in soil water content on the acclimation of tree species with distinct water use strategies. The results show that the deviations between measurements and predictions from the simplified optimality principle can explain different species' acclimation behaviors.

Keywords Abiotic stressors · Juniper-piñon pine woodlands · Plant carbon-water economies · Stomatal optimization theories

Introduction

Climate change is expected to increase the frequency and severity of both drought and heatwaves, especially in the temperate, semi-arid, and arid zones. Shifts in plant functioning and in turn in the tree and ecosystem-level water, carbon, and energy balances in association with drought and

rising temperature have already been documented in all major global biomes [1, 2]. As the climate warms, the evaporative demand will increase due to a higher vapor pressure deficit, leading to a greater loss of water from the soil and vegetation [3, 4], which will make these regions even more susceptible to drought. The fate of the current vegetation in these areas will depend on the ability of the species to tolerate and adapt to unprecedented conditions where higher temperatures leading to increased evaporative demand and “atmospheric drought” will coincide with a lack of precipitation and more frequent and severe “soil drought.” Generally, plants can adapt to new environments both structurally and functionally. Structural adaptations, such as increased root

Sanna Sevanto and Jean-Christophe Domec contributed equally to this work

✉ Mazen Nakad
mazen.nakad@gmail.com

Extended author information available on the last page of the article

growth to improve access to water and development of different leaf forms [5] and surface structures such as smooth or seriated leaves bearing waxy cuticles in conifers [6], or thick and hairy leaves with trichomes in angiosperms [7] to conserve water or reflect excess sunlight or reduction in xylem conduit diameter [8–10] as a response to increased solar irradiation and drought occur at time scales of years to decades [11]. Functional acclimation, such as biochemical changes in leaves to reduce photodamage under increased irradiation, on the other hand, can occur at time scales of several hours to days [12]. While adaptation and acclimation both contribute to plant survival in unprecedented conditions, the severity and time scale at which environmental changes occur will determine what amount of plasticity and at what time scale is required for survival.

Stomatal control of water loss is one of the main ways plants use to protect themselves from environmental stress such as drought. While stomatal closure is an effective mechanism to conserve water during drought, it comes with a cost of loss in photosynthetic productivity as stomatal closure prevents both exit of water vapor and entry of CO₂ for photosynthesis. This coupling of exit of water vapor and entry of CO₂ at stomatal level is the basis for the carbon-water economy coupling in plants. Different types of plants are known to vary in the sensitivity of stomatal conductance g to drought (soil drought) and heat (atmospheric drought) with consequences for their survival and growth [13]. Due to the rapid changes in leaf-to-air vapor pressure deficit, one of the key regulatory roles played by stomata is to limit transpiration-induced leaf water deficit. Plants that minimize water loss with increasing vapor pressure deficit and/or drought stress maintain a rather constant minimum leaf water potential and are termed as “isohydric” [14]. In isohydric plants, when drought pushes soil water potential close to this minimum leaf water potential, water can no longer be extracted, and the stomata close to prevent leaf desiccation. Plants that control leaf water potential less strictly have been termed as “aniso-hydric” [13]. Anisohydric plants allow leaf water potential to reach a less stable and much lower set point. This strategy produces a gradient in water potential between soil and leaf that allows gas exchange to continue over a greater decline in soil moisture and even under rising vapor pressure deficit [15, 16]. It is also shown that this classification is not a dichotomy but rather a continuum [17•]. The existence and co-dominance of both isohydric and anisohydric behaviors in many ecosystems have inspired a decade of research in how stomatal control strategies influence and could help predict tree mortality under drought [18, 19]. In terms of water and carbon economy, it has been argued that water use efficiency of isohydric plants should be higher than in anisohydric ones because their stomatal conductance and water loss are reduced quickly as soil dries [20], although there is evidence that anisohydric plants might have a higher specific photo-

synthesis rate than isohydric plants [21]. However, because of the non-linear shape of the CO₂ assimilation curve with water potential, isohydric plants are also expected to decrease their photosynthetic rate more slowly than stomatal closure, and thus, water use efficiency of isohydric species could potentially be more sensitive to environmental conditions than that of anisohydric species [21]. It is thus important to establish whether the way stomata control water potential allows plants to withstand more severe growing conditions by optimizing water loss over carbon uptake.

Interestingly, in many ecosystems, trees with different stomatal sensitivity to stresses co-exist or co-dominate. A case in point is the semi-arid Southwestern USA where piñon pine (*Pinus edulis* Englm.) trees co-dominate the ecosystems with a sympatric one-seed juniper (*Juniperus monosperma* Englm. (Sarg.)). Juniper keeps its stomata open further during more severe water stress than piñon pine allowing the persistence of more negative leaf water potentials [22]. Piñon pine on the other hand minimizes the increase in transpiration with increasing evaporative demand through a rather strong stomatal regulation of minimum leaf water status (water potential) despite large fluctuations in soil moisture content [14, 23, 24]. The isohydric stomatal behavior of piñon pine reduces photosynthesis and carbon uptake under drought, while the anisohydric strategy of one-seed juniper maintains photosynthesis and carbon assimilation at a higher rate during drought but potentially puts this species at a greater risk of hydraulic failure (cavitation-induced embolism) if drought is sufficiently intense to push soil water potentials below values that would induce xylem dysfunction [25, 26]. In contrast, stomatal closure at more negative water potentials in juniper did not necessarily impair hydraulic efficiency, due to its higher resistance to xylem embolism [27]. These types of isohydric and anisohydric species co-dominate many environments. Examples of co-dominant species in temperate forests include maple (isohydric), birch (isohydric), oak (anisohydric), and beech (anisohydric). In the boreal zone spruces, pines and firs belong to the isohydric end of stomatal control spectrum with larch and junipers following anisohydric strategy. Globally, isohydricity seems to be more prevalent in the boreal [28] and tropical [29] zones, while co-dominance of iso- and anisohydric species is common in the temperate zone [30, 31]. In terms of acclimation and adaptation, the co-dominance of (an)isohydric species raises the question of what would be the costs for species that maintain higher g and tolerate more negative leaf water potentials under future drought and rising temperatures? As well as, whether plants have the capability to switch from an anisohydric to an isohydric behavior so as to maximize carbon gain when soil moisture is available and limit plant desiccation when soil moisture is low [15, 32]? Some plant genera such as *Populus*, *Citrus*, and *Acacia* contain both iso- and anisohydric species [20, 33], and in grapevine, different cultivars can

show different stomatal responses to desiccation [34]. In the current absence of a scientific understanding of what triggers different stomatal behaviors, an alternative option to predict how plants can withstand changing abiotic conditions is to use model-based analysis of plant water and carbon economy within the framework of controlled experiments [35]. Manipulation studies offered compelling research data by allowing the control of multifactor climate conditions (e.g., drought, temperature) [36, 37••]. In addition, mechanistic insights from models can be monitored with respect to time along with changes in the environment affecting the stresses imposed. This merger allows hypotheses to be generated that cannot be directly tested in natural settings.

In this review, the background for using optimality theories to understand plant function is first considered. Next, a case study from an ecosystem-scale climate manipulation experiment is employed to re-examine plant gas exchange data. In this experiment, drought, heat, and combined drought and heat treatments were employed on juniper-piñon pine woodland in the Southwestern USA. This case study seeks to illustrate the use of optimality theories so as to shed light on the connection between the plant water and carbon economy and the differences in acclimation resulting from iso- and anisohydric stomatal control in co-occurring isohydric piñon pine and anisohydric one-seed juniper. In particular, the basic premises of this theory are covered, and the most elementary version of the widely accepted stomatal optimality theory is used. This theory, known as the “diffusive conductance theory or photosynthesis-stomatal conductance theory,” suggests that plants regulate stomatal aperture to balance the trade-off between maximizing carbon dioxide uptake for a given water loss [38, 39, 40••]. After this theory is reviewed, modeled changes in environmental conditions alone are contrasted against changes in environmental conditions accompanied by acclimation. This contrast seeks to explain the behavior of stomatal conductance for the two “end-member” stomatal control strategies in stressed environments with and without acclimation.

Methods

There are two guiding principles to the approach used for addressing the questions posed here. The first is motivated by the mathematician Pierre Louis Maupertuis (1698–1759) while the second closely follows the mathematician and computer scientist Seymour Papert [41]. Maupertuis is credited for developing the principle of least action in physics, which set the stage later on for the derivation of the Euler-Lagrange equation and their solution using the calculus of variation. The principle of least action was shown to recover all Newtonian mechanics and is the most comprehensive principle in

physics. While elementary aspects of the calculus of variation will be followed here for representing g , it is Maupertuis “portal” into the future that sets the stage for the review. This stage is best summarized in Maupertuis’ own words when assessing the consequences of the principle of least action:

“The laws of movement and of rest deduced from this principle being precisely the same as those observed in nature, we can admire the application of it to all phenomena. The movement of animals, the vegetative growth of plants ... are only its consequences; and the spectacle of the universe becomes so much the grander, so much more beautiful, when one knows that a small number of laws, most wisely established, suffice for all movements.”

The complexity sought for representing g (i.e., stomatal movement, which defines stomatal conductance) follows the framework of mind-sized bites set by Papert [41]. Mind-sized bites models are not necessarily targeting predictions per se (although they can) but are intended for understanding the relation between cause and effect in simple (i.e., few elements), realistic (i.e., preserves known laws), structured (i.e., composed of basic building blocks), and testable manner [42]. Thus, the approach for representing g here can be viewed as a continuation of Maupertuis’ project on movement (stomatal kinetics here) with model developments routed in mind-sized bites. Optimality principles derived from calculus of variation are gaining traction in the ecological sciences to seek extra mathematical constraints on missing processes given the complexity and knowledge gaps in such systems [43]. Before presenting these optimality principles, a historical overview of key developments of stomatal conductance modeling is presented.

Brief Historical Overview

The topic of stomatal movement and its relations to environmental stimuli is vast and cannot be covered in a single sub-section. The overview here is only offered to illustrate key mathematical models describing variations in stomatal conductance in response to micro-climate and draws upon a number of reviews and textbooks [44–46, 47•, 48, 49•, 50–52]. That micro-climate, especially its aridity, impacts stomatal aperture has already been recognized by Darwin [53]. Francis Darwin, the son of Charles Darwin, used a hygroscope to measure the aridity of the air and observed the closure of stomata on leaves when the atmosphere was dry. This led Darwin to conclude the following:

“when we remember the innumerable adaptations which serve to economize water, it is inconceivable that the closure of the stomata should not cooperate.”

The link between photosynthesis and transpiration was also a subject of intense studies, especially in the early 1920s by Scarth [54], who noted the following:

“when stomata regulate one process they must regulate the other also but the question remains as to which of these actions represents the real role of the stomata in the economy of the plant.”

Around that time, Bowen [55] showed how evaporation from lakes or open water bodies can be determined from the energy balance and micro-meteorological conditions (i.e., vertical gradients in the mean air temperature and water vapor concentration). Bowen’s work set the stage for the development of the Penman “combination equation” for evaporation from wet surfaces in the late 1940s, which combined atmospheric aridity (or the drying power of the atmosphere) with available energy [56]. It was Monteith [57] that revised Penman’s work in the mid-1960s to include a stomatal conductance term in the combination equation, thereby offering a blue-print on how to mathematically unite physics (energy balance, turbulent transport theories for determining the Bowen ratio) and physiology (stomatal conductance). Versions of what is now termed as the Penman-Monteith equation were later adopted by the Food and Agricultural Organization and remain in use today (see FAO manual, Ch.2). The attention to the stomatal conductance term in the combination equation lead to numerous empirical equations—the most common is due to Jarvis [58] proposed in the mid-1970s. The Jarvis model [58] represented stomatal conductance as a maximum value (presumed to occur when stomatal aperture is fully open) reduced by non-linear factors that depend on vapor pressure deficit, photosynthetically active radiation, carbon dioxide concentration, leaf water potential, and air temperature. These empirical functions enabled comparisons across species and led to some “functional” classifications of them such as shade-tolerant or drought-resistant species.

After Farquhar and co-workers [48] introduced the widely used photosynthesis model in the late 1970s, it was combined with Fickian mass transport for water vapor and carbon dioxide along with other extra empirical equations such as the Ball-Berry (e.g., [59]) or the Leuning equations [60] to predict many of the light and temperature responses of stomatal conductance. These extra empirical equations, developed in the late 1980s, primarily assumed that leaf stomatal conductance is proportional to photosynthesis but reduced by atmospheric carbon dioxide concentration and another empirically specified atmospheric aridity index based on either air relative humidity [61] or vapor pressure deficit [60]. The combined use of the Farquhar photosynthesis equation, a mass transfer equation, and one of the empirical relations (e.g., Ball-Berry or Leuning) were then introduced in climate models by the mid-1990s. This photosynthesis-stomatal conductance approach constituted one of the first attempts to

“green” climate models [62]. The mathematical form of these models remains in use today within many climate centers.

That stomatal conductance may, in fact, have a “universal” response to vapor pressure deficit changes was established in the late 1990s [63•] and verified on some 40 species. Attempts to explain this universal character from plant hydraulics later followed [64, 65]. In parallel, stomatal optimality theories (to be reviewed later) were gaining attention in the 1970s after the work of Cowan and Troughton [40••], Cowan [66], Cowan and Farquhar [67], Givnish [38], and many others [68–72]. Attempts to derive the universal response of stomatal conductance to vapor pressure deficit from such optimality principles was then established [70, 73] followed by similar attempts to derive the family of functions codified by the Ball-Berry and Leuning formulations (and their aridity index) from similar approaches [74–76].

A missing gap remains regarding soil moisture dynamics, elevated temperature, and their interactive effects, which frames the scope here. Regarding soil moisture stress, early attempts assumed that the empirical parameters of the Ball-Berry or the Leuning formulations for g vary with leaf water potential [77] or simply soil moisture [78]. However, progress in combining dynamic soil moisture with optimality theories commenced with the pioneering work of Cowan [79] and others [39]. These attempts later inspired the use of dynamic optimality theories [80, 81••] and other game-theoretic principles with legacy effects included [82]. However, the combination of thermal and soil moisture stress and their interactive effect on stomatal conductance has not been tackled by such optimality principles. This review focuses on this issue with a lens on how isohydric versus anisohydric strategies impact stomatal response to drought, heat stress, and combined drought and heat stress.

Formulating the Optimality Principle

Stomatal optimality theories are premised on stomatal aperture opening to *maximize* carbon gain (needed for reproduction, survival, and plant defenses) for a given amount of water available in the soil per unit leaf area [38, 40••, 68, 72, 81••, 83]. This theory is presumed to be general and applicable to most species, including the juniper-piñon pine woodland considered here. In the process of uptaking a single carbon dioxide molecule, plants lose some three orders of magnitude more water molecules (transpirational cooling) that reduces leaf heat stress. When the working assumption is that every carbon dioxide molecule that enters the sub-stomatal cavity is assimilated (i.e., steady-state conditions), the carbon gain per unit leaf area per unit time can be represented by the photosynthetic rate (f_c). Hence, stomatal optimization seeks to quantify the optimal path to be followed by g for opening and closing of the stomatal aperture in time t so as to maximize the carbon gain during a certain pre-defined period T_p .

Mathematically, g should adjust over a time period T_p so that [80, 81••]

$$L_o = \int_0^{T_p} f_c(g)dt, \tag{1}$$

where t is time, T_p is taken as the interpulse duration between rainfall events, and L_o is the objective function to be maximized by g variations in t . Without any additional constraints, it can be argued that stomata should remain open to a maximum allowed by their structural properties (e.g., fully open aperture) so that $g = g_{max}$. Derivations that link g_{max} to stomatal and leaf geometry as well as ventilation and vapor interference across pores is a maturing field that can be employed here [84]. However, there are numerous constraints on this maximization that prevent $g = g_{max}$ to operate at all times. Soil water availability is a logical one to employ (especially here) given the voluminous loss of water molecules incurred in the process of gaining a single carbon dioxide molecule. Hence, a minimalist constraint is that the maximization of L_o must be subject to a water availability constraint in the root zone. Supposing that the initial amount of water in the rooting zone per unit leaf area is W_o above the wilting point, this W_o must then be sufficient to sustain photosynthesis over the time period T_p when g adjusts in t . Mathematically, this constraint may be expressed as [81••]

$$W_o = \int_0^{T_p} f_e(g)dt, \tag{2}$$

where f_e is the loss of water or transpiration from leaves per unit leaf area. Once again, this loss of water can be regulated by g . To solve this “constrained optimization” problem for L_o subject to the constraint in Eq. 2, a Hamiltonian (H) can be written as [68, 81••]

$$H = f_c(g) - \lambda f_e(g), \tag{3}$$

where λ is referred to as the marginal water use efficiency or the Lagrange multiplier of the optimization problem. The ecological significance of the Lagrange multiplier here is that it measures the cost of losing a water molecule to the carbon economy of the plant. The solution for L_o subject to the constraint in Eq. 2 can be derived using the calculus of variation by solving the Euler-Lagrange equation [85]

$$\frac{d}{dt} \left(\frac{\partial H}{\partial \dot{g}} \right) - \frac{\partial H}{\partial g} = 0, \dot{g} = \frac{dg}{dt}. \tag{4}$$

Since H in Eq. 3 does not explicitly depend on \dot{g} , all partial derivatives of H with respect to \dot{g} are set to zero and the

Euler-Lagrange equation reduces to

$$\frac{\partial H}{\partial g} = \frac{\partial f_c(g)}{\partial g} - \frac{\partial \lambda f_e(g)}{\partial g} = 0. \tag{5}$$

When the time variations in g (usually minutes) are occurring on time scales much faster than the variation in root-zone soil water (usually days), λ may be momentarily “arrested” for a short amount of time so that

$$\frac{\partial H}{\partial g} = \frac{\partial f_c(g)}{\partial g} - \lambda \frac{\partial f_e(g)}{\partial g} = 0. \tag{6}$$

As soil moisture is depleted, λ can be allowed to vary slowly with root-zone soil moisture content, which will be used here as a working assumption for simplicity [80]. In some studies, Eq. 6 was used to define λ , and variability in computed λ was deemed as evidence that plants are not operating optimally [86].

Using the Optimality Principle

To utilize the Euler-Lagrange formulation in Eq. 6, it is necessary to express f_c and f_e as functions of the “control variable” $g(t)$ regulated by plants. For C3 plants, the biochemical demand for CO₂ is described by the Farquhar photosynthesis model [87••] expressed as

$$f_c = \frac{\alpha_1}{\alpha_2 + c_i} (c_i - c_p), \tag{7}$$

where c_p is the CO₂ compensation point, α_1 and α_2 are two photosynthetic parameters selected depending on whether the photosynthetic rate is RuBP (ribulose biphosphate) or RuBisCo (Ribulose-1,5-bisphosphate carboxylase-oxygenase) limited, and c_i is the intercellular CO₂ concentration. Equation 7 assumes that the contribution of dark respiration to f_c is negligible, which is the case for high photosynthetic periods during the day. Equation 7 can be further simplified by its linear part when $c_p \ll c_i$ and the variability of c_i in the denominator of Eq. 7 are small. This assumption is likely to hold for RuBisCo limitations. In this case, α_1 can be approximated by the maximum carboxylation capacity V_{cmax} and $\alpha_2 = K_c(1 + O_a/K_o)$, where K_c and K_o are the rate constants for CO₂ fixation and oxygen inhibition and O_a is the oxygen concentration in air. Hence, variations in c_i (usually of order 30 ppm) are now presumed to be small compared to α_2 (usually of order 550 ppm). Table 1 shows the definitions of these parameters and their temperature dependence. With this linearization to the $f_c - c_i$ curve in the denominator, the biochemical demand reduces to

$$f_c = \frac{\alpha_1 c_i}{\alpha_2 + s c_a} \tag{8}$$

Table 1 List of the the C3 photosynthetic model parameters (i.e., $f_c - c_i$ curve) and their respective temperature (T) adjustments

Parameter	Value or temperature adjustment	Units
$\alpha_1 = V_{cmax}$	$V_{cmax,25} \exp[m_1(T - 25)][1 + \exp[m_2(T - 41)]^{-1}$	$\mu\text{mol m}^{-2} \text{s}^{-1}$
α_2	$K_c(1 + O_a/K_o)$	$\mu\text{mol m}^{-2} \text{s}^{-1}$
K_c	$K_{c,25} \exp[0.074(T - 25)]$	$\mu\text{mol mol}^{-1}$
K_o	$K_{o,25} \exp[0.018(T - 25)]$	$\mu\text{mol mol}^{-1}$
$K_{c,25}$	300	$\mu\text{mol mol}^{-1}$
$K_{o,25}$	300	mmol mol^{-1}
O_a	190	mmol mol^{-1}
$V_{cmax,25}$	Fitted based on treatment	$\mu\text{mol m}^{-2} \text{s}^{-1}$
m_1 and m_2	Fitted based on treatment	$^{\circ}\text{C}^{-1}$

where c_a is the atmospheric CO₂ concentration and $s = 0.7$ based on long-term mean c_i/c_a (ensemble-averaged for C3 plants) based on numerous studies [49]. This simplification reproduces comparable results to the nonlinear model of Eq. 7 as shown in previous studies [75, 88] for RuBisCo limitations. However, this linearization leads to a “mind-sized bite” model for g , which can be used to quantify plant acclimation and responses to different abiotic factors.

The atmospheric supply of carbon dioxide and associated plant water vapor loss to the atmosphere can be described by Fickian diffusion through stomatal pores and are given by

$$\begin{aligned} f_c &= g(c_a - c_i) \\ f_e &= ag(e_i - e_a) \approx agD, \end{aligned} \quad (9)$$

where g is interpreted here and throughout as the stomatal conductance to CO₂, $a = 1.6$ is the relative molecular diffusivity of water vapor with respect to carbon dioxide, e_i and e_a are the intercellular and ambient water vapor concentration respectively, and D is the vapor pressure deficit that is approximated as $e_i - e_a$, which is only valid when the leaf is well coupled to the atmosphere. In Eq. 9, the atmospheric supply of carbon dioxide neglects the mesophyll pathway that can be significant under certain circumstances [88, 89]. In this case, the mesophyll conductance is infinite, and the chloroplastic CO₂ concentration c_c is approximated by the intercellular CO₂ concentration c_i . This might not be the case during drought conditions where the mesophyll conductance might be more limiting than g . However, the inclusion of the mesophyll conductance using simplified models described elsewhere [88] that represent c_c/c_i as a function of soil moisture had a minor impact on the results (not shown) and not featured for simplicity. Combining Eqs. 8 and 9 yields the sought $f_c(g)$:

$$f_c = \frac{g\alpha_1 c_a}{\alpha_1 + g(\alpha_2 + sc_a)}. \quad (10)$$

Before proceeding further, a number of comments about Eq. 10 are in order regarding the general role of g and c_a .

The first is that as c_a becomes very large (exaggerated here by allowing $c_a \rightarrow \infty$) but $g > 0$, f_c saturates to α_1/s and does not monotonically increase. Thus, $\alpha_1 = sf_{c,max}$ may be viewed as setting an upper bound on how much the biosphere can absorb atmospheric carbon dioxide per unit leaf area provided $g > 0$. At high g (exaggerated again by allowing $g \rightarrow \infty$) but finite c_a ,

$$f_c = \alpha_1 \left[\frac{c_a}{(\alpha_2 + sc_a)} \right]. \quad (11)$$

For a $c_a = 550$ ppm, $\alpha_2 = 550$ ppm, and $s = 0.7$, $f_c/f_{c,max} = 0.58$. When removing stomatal limitations on photosynthesis, c_a becomes the limiting resource—and even for an elevated $c_a = 550$ ppm, $f_c/f_{c,max}$ remains only at about 0.6. Naturally, these limiting cases must be treated with caution as the linearized biochemical demand may not hold for very high c_a ; however, RuBisCo limitations may still set an upper bound on f_c in such cases. Specifically, extrapolating a linear $f_c - c_i$ to high c_i (as is expected from RuBisCo limitations) overpredicts f_c compared to a saturation limit set by RuBP regeneration.

Solving for the Optimal Conductance

Assuming $g > 0$ (i.e., stomates are open), replacing Eqs. 10 and 9 into Eq. 6, and solving for g yields

$$g = \frac{\alpha_1}{\alpha_2 + sc_a} \left[-1 + \left(\frac{c_a}{a\lambda D} \right)^{1/2} \right]. \quad (12)$$

In general, λ can be determined from the constraint in Eq. 2. Operationally, implementing this constraint for time-dependent D , air temperature, and soil water content and for variable T_p along with stochastic W_o proves to be challenging [80, 81]. In practice, λ is treated as a fitting parameter to be determined and assumed to reflect the cost of losing water in carbon units. Notwithstanding this difficulty, different environmental factors that affect g can still be studied.

For example, water availability in the rooting zone is embedded in λ , and the temperature effects can be accommodated through the photosynthetic parameters α_1 and α_2 as shown in Table 1. While the approach here ignored dark respiration, assumed that $c_p/c_i \ll 1$, and linearized the $f_c - c_i$ biochemical demand function, the complete solution for g (labeled g_{full}) has been derived (analytically) when relaxing these assumptions and is given by [75]

$$\frac{g_{full}}{\alpha_1} = \frac{-(\alpha'_2 - 2c_a + 2c_p)}{(\alpha'_2)^2} + \frac{\sqrt{\lambda_u (c_a - c_p) (\alpha_2 + c_p) (\alpha'_2 - 2\lambda_u)^2 (\alpha'_2 - \lambda_u)}}{\lambda_u (\alpha'_2)^2 (\alpha'_2 - \lambda_u)}, \tag{13}$$

where g_{full} is the stomatal conductance derived for the non-linear $f_c - c_i$ biochemical demand function including the compensation point c_p , $\lambda_u = a\lambda D$, and $\alpha'_2 = \alpha_2 + c_a$. The simpler expression given in Eq. 12 will be used throughout for simplicity unless otherwise stated.

Emergent Properties from Optimality Theory

The simplified optimality theory here establishes a relation between cause and effect in simple (i.e., minimal number of variables), realistic (i.e., preserves known mass transfer laws such as Fickian diffusion and physiological principles such as the $f_c - c_i$ relation for C3 plants), structured (i.e., composed of basic building blocks), and testable, which is the subject of this sub-section. To begin, the simplified optimality theory in Eq. 12 recovers several complex features about stomatal regulation (not originally assumed) and many empirical results regarding the relation between photosynthesis and g . Those features are now reviewed.

Sensitivity of g to Atmospheric Aridity

A widely used empirical formulation for g is given by [63•]

$$\frac{g}{g_{ref}} = 1 - m \ln(D), \tag{14}$$

where m was shown to be approximately constant with values ranging between $m=0.5$ and $m=0.6$, and g_{ref} is a reference conductance defined at $D = 1$ kPa, high light levels, and high soil moisture content. Equation 14 has received broad experimental support in the literature at several scales spanning leaf gas exchange, sap flow time series, and eddy-covariance latent heat flux measurements [63•, 65, 90, 91]. Thus, Eq. 14 may be viewed as a summary of a large corpus of experiments covering some 80 species. As reviewed elsewhere [73], this model can be reconciled with optimality arguments when noting that $D^{-1/2}$ can be expanded in a Taylor series

around $D = 1$ kPa with the two leading order terms being $1 - (1/2) \ln(D)$.

One puzzling feature about stomatal responses to D variation is the so-called apparent feedforward mechanism [45, 92•]. This mechanism, which was not assumed in the stomatal optimization framework, is labeled as such because plants appear to shut down their stomata faster than the increase in the driving force for leaf transpiration (i.e., D). This rapid closure provides the appearance that stomates are anticipating occurrences of high atmospheric aridity and thus close faster than the driving force for $f_e \propto D$ to conserve water with increasing D . This topic has received significant attention since the early 1970s [45, 73, 93–97]. Some studies argue that this response is an artifact of the temperature sensitivity of photosynthetic parameters [98]. Others have shown that for RuBisCo limited photosynthesis, and even when accommodating these temperature effects, the apparent feedforward mechanism still emerges albeit at a weaker level than earlier field experiments suggested when field data are not binned by temperature increments [99]. Mathematically, as D increases, the point at which the apparent feedforward commences can be derived from the f_e versus D relation. At the incipient D of the apparent feedforward, $\partial f_e / \partial D = 0$ despite the fact that g monotonically declines with increasing D [73]. The emergence of the coefficient -1 in Eq. 12 is the main cause for the existence of such an apparent feedforward mechanism (or anticipatory response by the stomates), and this term is an emerging outcome of the optimality theory. The D at which the apparent feedforward mechanism commences with increasing D (i.e., $\partial f_e / \partial D = 0$) can now be computed and given as $D_{afm} = (4/9)(c_a/a)\lambda^{-1}$. That is, the D at which the apparent feedforward mechanism can be expected varies with W_o or λ and c_a . Equation 14 also predicts an apparent feedforward mechanism for D exceeding $D_{afm} = \exp[(1 - m)/m]$. This finding is dynamically interesting because it enables a link between m and λ given by

$$\lambda = \frac{4}{9} \frac{c_a}{a} \exp\left[\frac{m - 1}{m}\right], \tag{15}$$

and suggests that λ increases linearly with increasing c_a for constant m as demonstrated elsewhere for other theories [80] and experiments [76, 83]. Equation 13 also suggests that an apparent feedforward mechanism emerges only when

$$C_{afm} = \frac{-(\alpha'_2 - 2c_a + 2c_p)}{(\alpha'_2)^2} < 0. \tag{16}$$

For RuBP regeneration limitations on f_c , $\alpha_2 + 2c_p$ is small compared to current and future c_a making $C_{afm} > 0$. The opposite is likely for RuBisCo limitations on f_c , where α_2 can exceed c_a . Thus, it may be conjectured that the apparent feedforward mechanism is likely to occur for RuBisCo

limitations and not RuBP regeneration limitations on f_c . For example, a simplified (and popular) solution to the optimality problem assuming RuBP regeneration limitations to f_c [74] cannot reproduce the apparent feedforward mechanism. Moreover, for any given instant, C_{afm} varies with photosynthetically active radiation, temperature, and c_a .

Recovering Empirical Models for g

Empirical formulations for g used in climate models are commonly expressed as

$$g = m'' \left(\frac{f_c}{c_a} \right) F_A, \quad (17)$$

where m'' is a species-specific sensitivity parameter presumed to vary with soil moisture or leaf water potential [78], and F_A is a dimensionless function of atmospheric aridity. Some models set $F_A = RH$ [59] while others set $F_A = (1 + D/D_o)^{-1}$ [60] where RH is the air relative humidity and D_o is a species-specific empirical coefficient. The mathematical form of Eq. 17 has been shown to describe a large number of leaf gas exchange measurements across numerous species [60] and climatic conditions [100] and may be viewed as a compact summary of all these experiments [59]. Despite differences in F_A , these (and many other) empirical models suggest a robust near-linear relation between g and f_c/c_a . Thus, it is instructive to ask whether optimality theory can recover these formulations [74, 75]. Upon inserting Eqs. 12 into 10 and simplifying, it can be shown that

$$g = \left(\frac{f_c}{c_a} \right) \sqrt{\frac{c_a}{a\lambda}} D^{-1/2}. \quad (18)$$

The $D^{-1/2}$ scaling and the linearity between g and f_c/c_a both emerge from the optimality arguments and are not a priori imposed or assumed [68, 73]. Moreover, when the findings in Eq. 15 are combined with Eq. 18, the resulting outcome offers a new perspective on m'' . These combined equations yield

$$g = m' \left(\frac{f_c}{c_a} \right) D^{-1/2}, \quad m' = \sqrt{\frac{9}{4} \exp\left(1 - \frac{1}{m}\right)}, \quad (19)$$

where m' may be treated as a constant when m is constant. When m varies with soil moisture, m is expected to decline as has been shown using hydraulic models and a wide array of flux measurements across biomes [65]. Hence, the simplified optimality argument here can be reconciled with prior empirical stomatal conductance models [47, 59]. Such reconciliation is not limited to RuBisCo (the case here) but also

emerges for RuBP regeneration limitation on photosynthesis [74].

Sensitivity of Water use Efficiency to Atmospheric Aridity

The simplified optimality model predicts an optimal c_i/c_a associated with the optimal g given by

$$\frac{c_i}{c_a} = 1 - \sqrt{\frac{a\lambda}{c_a}} D^{1/2}. \quad (20)$$

A large number of experiments and empirical models show that as D increases, c_i/c_a decreases non-linearly [73, 101, 102]. Similarly, decreases in soil moisture lead to increases in λ and concomitant increases in c_i/c_a as expected [102]. The optimal c_i/c_a leads to an optimal water use efficiency WUE given by

$$WUE = \frac{f_c}{f_e} = \frac{(c_a)(1 - c_i/c_a)g_s}{aDg_s} = \frac{c_a}{(aD)^{1/2}} \sqrt{\frac{\lambda}{c_a}}. \quad (21)$$

Once again, increases in c_a , declines in D , and declines in root-zone soil moisture resulting in increases in λ all lead to increases in water use efficiency consistent with logical expectations [102]. For a near constant m , Eq. 15 suggests that $\lambda \propto c_a$ and

$$WUE = \frac{2}{3} \frac{c_a}{a\sqrt{D}} F_1(m); \quad F_1(m) = \sqrt{\exp\left(1 - \frac{1}{m}\right)}, \quad (22)$$

where $F_1(m)$ is bounded between $F_1(0.5) = 0.6$ and $F_1(0.6) = 0.7$. This finding explains why in well-watered soil moisture conditions (i.e., constant m), $WUE \propto c_a$ and $WUE \propto D^{-1/2}$ as reported for numerous studies reviewed elsewhere [73]. The $D^{-1/2}$ scaling was shown to be the best descriptor (statistically) across all FluxNet eddy-covariance sites for ecosystem level WUE [103]. It is for this reason that $WUE \propto D^{-1/2}$ is used to partition evapotranspiration (ET) into its two components [104–106]. These partition predictions of ET have also been confirmed using independent methods, where the $D^{-1/2}$ scaling emerged in the WUE [107]. Last, Eq. 21 also links the water use efficiency to the marginal water use efficiency and can be used to set bounds on λ .

The Hamiltonian and Halox Experiments

Similarities in representing the cost of losing water to the carbon economy as λf_e and the findings from Halox (Helium/oxygen mixture) gas experiments [108] are now pointed out. These experiments are based on the fact that water vapor diffuses about 2 times faster in Helox than in air.

Hence, the water vapor concentration difference between the leaf and the air at the leaf surface can be experimentally varied independent from the transpiration rate and vice versa. These experiments showed that stomata did not directly sense or respond to either the water vapor concentration at the leaf surface or the difference in water vapor concentration between the leaf interior and the leaf surface. The main mechanism responsible for stomatal closure as a function of varying humidity was the rate of water loss itself accompanied by reductions in f_c even when c_i was held constant. These results are consistent with Eq. 18 derived from the Hamiltonian in Eq. 3.

Other Optimality Theories

The finding in Eq. 12 may be viewed as appropriate when water availability sets the constraint (i.e., W_o). There are numerous instances where both access to water and transmission of water in the plant system impose severe constraints [81••]. In those cases, representing the (i) rhizospheric controls on soil water access [109–112] and (ii) plant hydraulics (i.e., organ wide vulnerability curves) on water transmission becomes necessary [81••, 113, 114]. Given the proliferation of hydraulic traits, a number of extensions have been proposed when water transmission is limited. Notably, those approaches are now labeled as “profit maximization” [115–117]. They argue that evolutionary strategies in water-competitive environments lead to the maximization of carbon gain *minus* hydraulic risk. This approach proved effective in explaining broad patterns of hydraulic failure in woody plants [116]. Other variants consider the effects of water stress directly on leaf photosynthesis by adding a mesophyll conductance thereby linking leaf water potential to photosynthesis [88, 118]. Water moves in leaves through xylem conduits within the veins and, once passed the bundle sheath, is transported through the mesophyll cells. This outside-xylem pathway is sensitive to cell water content and water potential [119]. In these models, the cell carbon dioxide concentration (c_c) deviates from c_i due to the presence of a mesophyll conductance, and c_c/c_i is presumed to vary with leaf water status. Evidence from drought and salt-stress experiments supports these simplifications [89, 118]. Another line of inquiry is that during drought, sucrose transport in the phloem becomes the constraining factor to photosynthesis. To maintain osmoregulation, large amounts of sucrose are needed to ensure sufficient driving force for water and sugars. However, at high sugar concentration, the water viscosity increases rapidly thereby resisting the driving force [120]. Thus, the objective function becomes sucrose transport maximization instead of carbon uptake maximization by leaves. In this framework, plants regulate leaf water potential to maximize sucrose transport from the source (leaf) to the sink (root) as featured elsewhere [121–125]. Another

perspective argues that leaves minimize the summed unit costs of transpiration and carboxylation [126]. This approach recovers results similar to those featured here but using an entirely different objective function. To sum up, the studies listed here are by no means an exhaustive list. They are selected because they arrive at mathematical models that share some resemblance to those presented here and may be summarized as

$$\frac{\partial}{\partial y} H_{eff} = \frac{\partial}{\partial y} (Ga - \lambda_{eff} Lo), \quad (23)$$

where H_{eff} is the objective function to be extremized (e.g., the Hamiltonian here), y is the control variable by the plant (i.e., g for the approach here or leaf water potential in the profit maximization), Ga is a gain (often linked to the carbon economy of the plant), Lo is a loss (related to water availability, water access, or transmission), and λ_{eff} is a conversion factor (e.g., Lagrange multiplier) linking the costs to the carbon economy of the plant. In the profit maximization approach, for example, it is set to unity because Ga and Lo are expressed as relative gains and relative losses. A subset of the aforementioned models have been compared against several data sets with results that are qualitatively similar even for other stresses such as salinity [127].

Re-examining Recent Field Experiments

Thus far, the optimality theory was explored in the context of a universal response of g to D , how elevated atmospheric carbon dioxide may impact λ , and the emergence of a linear $g - f_c/c_a$ relation. The work also highlighted connections between λ and water stored in the rooting zone via the constraint in Eq. 2. The findings from optimality theory can be used to interpret numerous leaf gas exchange experiments across many C3 species. Next, the interactive effects of drought and warming at longer time scales are to be considered. These interactive effects and their connection to iso-hydricity remain a frontier in ecology. To address the “data gap,” a unique experiment was conducted at the Los Alamos Survival-Mortality (SUMO) site [37••] and is now re-interpreted using optimality theory. Briefly, the site is composed of two different species expressing isohydric (in this case piñon pine) and anisohydric (in this case juniper) stomatal behavior. The trees were assigned to four different treatments: (i) ambient conditions (A) representing a semi-arid climate (i.e., the climate of the site location), (ii) heated conditions (H) where air temperature was maintained at 4.8 °C above ambient air temperature using air-conditioned open-top chambers, (iii) drought conditions (D) where trees experienced a 45% precipitation reduction obtained covering the area with plastic troughs that diverted precipitation away from the site, and (iv) heat and drought conditions

(H+D) where both treatments were applied simultaneously. The data collected included time series of sap flux density (FD), mean air temperature (T), mean vapor pressure deficit (D), and mean relative extractable water (REW) calculated from soil moisture content data [37••]. The duration of the experiment was 200 days starting from March 1st to September 18th of 2016. All data were publicly available as daily averages, and the vapor pressure deficit was divided by the atmospheric pressure (based on temperature and site location) for unit conversion (unitless D is needed in the g model). Since this long-term experiment provided only daily averaged temperature values that include nighttime, the average daily temperature was increased by 20% to reflect mean daytime temperature needed in the photosynthesis calculations.

Across treatments, there were no significant anatomical changes in lumen area, sapwood area to leaf area ratio, and wall thickness during the experiment [37••]. Much of the treatment effects within a species appeared to be in xylem hydraulic conductance, which impacts c_i/c_a (and λ) [128]. Since comparisons between the isohydric and anisohydric species are sought and only daily meteorological conditions and sap flow measurements are publicly available, the $f_c - c_i$ curve was presumed to be linear and given by Eq. 7. Physiologically, this simplification is akin to assuming f_c is RuBisCo limited. Light saturation were expected for most of the day given the geography of the site and the small size of the plants. The different parameters needed for g and the examination of acclimation are briefly reviewed. From Eq. 12, plant acclimation can be divided into two effects: (i) acclimation due to photosynthetic changes, which is related to changes in the maximum rate of carboxylation $\alpha_1 = V_{cmax}$ (and provided from separate studies), and (ii) acclimation due to water uptake strategies (i.e., plant hydraulics), which is related to the plant response to water availability and is embedded in how λ varies with soil water (to be inferred from the re-assessment of the experiments here). For simplicity, the $K_{c,25}$, $K_{o,25}$ and the coefficients in the exponentials shown in Table 1 are assumed to be unaffected by the treatment. However, for $\alpha_1 = V_{cmax}$, the net assimilation to intercellular CO_2 concentration curves at different temperatures have been measured in separate experiments and used to approximate $V_{cmax,25}$, m_1 and m_2 for each treatment. These parameters are shown in Table 2, and they are assumed to

be the result of acclimation due to photosynthetic response. Due to lack of leaf gas exchange data on the heat and drought conditions, it was further assumed that the drought photosynthetic parameters are more representative of these conditions in qualitative agreement with empirical findings from a prior study [37••].

For the hydraulic response, λ can be approximated by fitting it to the relative extractable water (REW) for different starting phases of rain event (i.e., W_o) for each rainfall duration T_p . In this case, the transpiration f_e (the sap flux density FD per unit leaf area) from Eq. 9 can be used to obtain the measured stomatal conductance g . Using the measured g , λ is then calculated from Eq. 12 using the fitted parameters from Table 2. Finally, the nonlinear regression toolbox in MATLAB is used to fit λ to REW .

To ensure that fitted parameters were reasonable, plausibility constraints were also enforced. First, the calculated conductance should be positive, and that leads to a weak constraint that $c_i/c_a > 0$. To make sure that this condition is uniformly enforced for all runs, $c_i/c_a > 0.3$ was imposed for both species where the value 0.3 was tuned for maximizing the number of days used in the analysis while minimizing an unrealistic lower limit on c_i/c_a . Also, to ensure that dark respiration does not play a role, a threshold should exist on the lower bound of c_i . Second, since RuBisCo limitations were assumed in the model derivation (i.e., linear $f_c - c_i$), another constraint should be imposed but this time on c_i/α_2 . Theoretically, the value c_i/α_2 should be less than unity, and this condition was satisfied for almost all the runs for anisohydric juniper. However, this was not the case for the isohydric piñon pine. Hence, the condition $c_i/\alpha_2 < 0.4$ was further imposed to ensure that the linearization remains adequate for the purposes of comparing across treatments. This means that light-saturated conditions may not have been met, and the full model in Eq. 13 may be needed for some of the days (including the RuBP limitation).

Results and Discussions

The optimality hypothesis is now used to demonstrate the use of this framework to address the study objectives using the aforementioned experiments, literature survey, and

Table 2 Published photosynthetic parameters used for the linearized $f_c - c_i$ biochemical demand function

	Piñon pine			Juniper		
	Ambient	Heat	Drought	Ambient	Heat	Drought
$V_{cmax,25}$	34.5	31.8	27.0	54.3	50.9	43.8
m_1	0.073	0.069	0.096	0.094	0.091	0.090
m_2	0.23	0.11	0.20	0.15	0.17	0.10

The units of $V_{cmax,25}$, m_1 and m_2 are $\mu mol m^{-2} s^{-1}$ and $^{\circ}C^{-1}$ respectively as shown in Table 1

independent gas exchange measurements. Again, the goal here is not to model all the details of g but to compare the g across treatments for each species. The computed λ for the two species are first presented and compared. Throughout this section, the stomatal conductance g has the following unit $mmol\ m^{-2}s^{-1}$ and water use efficiency λ is unitless, respectively. All other units for the constants are shown in Table 1.

Model Parameters

Figure 1 a and b show the results for the fitted λ as a function of REW for piñon pine and juniper, respectively. Interestingly, the λ for piñon pine did not vary appreciably across treatment whereas, for the anisohydric juniper, the variations were more pronounced for ambient and heated (0.006–0.01) conditions. Recall that $g \propto \lambda^{-1/2}$ further ameliorating the differences for piñon pine ($0.004^{-1/2}=15.8$, $0.006^{-1/2}=13$) and to a lesser extent juniper ($0.008^{-1/2}=11.2$, and $0.01^{-1/2}=10$). Another interesting observation regarding the magnitude of λ is that juniper λ had a higher maximum value compared to piñon

pine. This again shows the difference between anisohydric and isohydric behaviors where the cost to extract water is higher for juniper compared to piñon pine. The supplementary Figs. S1 and S2 show the fitted and measured λ as a function of REW for piñon pine and juniper respectively. The supplementary Table S1 shows the performance of the fitted data for λ .

Figure 2 a and b compare the measured and modeled g for piñon pine and juniper, respectively. The calculated and measured g reasonably agree despite the model simplicity. The supplementary Table S2 shows the performance of the fitted data for g .

Evaluating Photosynthetic Acclimation

Having demonstrated that the optimality hypothesis reasonably recovers g , it is now used to separate the different strategies plants use to acclimate to a changing environment. As discussed earlier, the effects of acclimation on the photosynthetic machinery can be detected in the maximum carboxylation rate. In this case, one can analyze the changes in the photosynthetic parameters for each treatment and how it affects g . To do so, g was calculated using the photosynthetic parameters of the ambient conditions, which are provided in Table 2, while accounting for the water use efficiency by using the fitted λ for each treatment. This allows discerning acclimation on carbon assimilation alone and its effect on g . Figures 3 a and b show these results for piñon pine and juniper respectively. In these figures, g with acclimation is calculated from the fitted parameters as discussed in “Re-examining Recent Field Experiments” section and plotted against g without acclimation, which is the calculated g using the photosynthetic parameters for ambient conditions as discussed earlier, for different treatments.

The deviation from the one-to-one line highlights the effect of acclimation of photosynthetic parameters on g . As one can see from these figures, both species behaved in a similar manner during combined drought and heat and drought-only conditions where they decreased their g to acclimate to a changing environment. However, under heated conditions only, juniper was able to maintain the same g , which was not the case for piñon pine. As shown in Fig. 3a, g of the isohydric piñon pine had to decrease by 19% for heated conditions, 32% for drought conditions, and 26% for heat and drought conditions. On the other hand, g of the anisohydric juniper decreased by only 2% for heated conditions, 20% for drought conditions, and 22% for heat and drought conditions (Fig. 3b). These percentages were similar for drought and heat-drought conditions, which might reflect the assumptions of using the same photosynthetic parameters for both conditions. The supplementary Table S3 shows the deviation statistics for all treatments and both species.

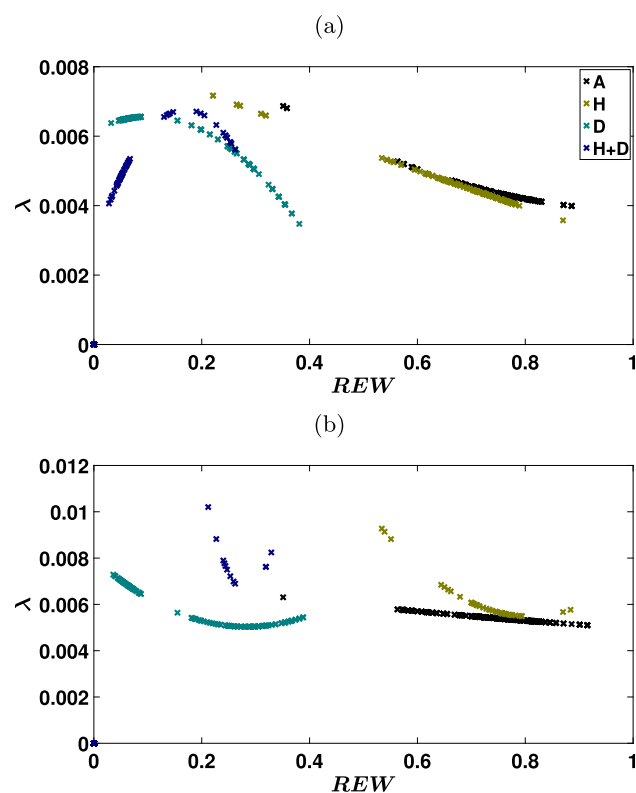
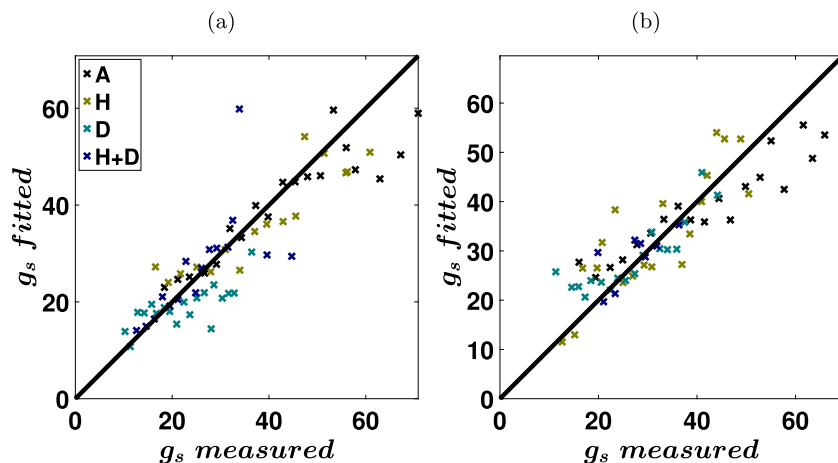


Fig. 1 Fitted marginal water use efficiency λ as a function of relative extractable water (REW) for **a** piñon pine (isohydric) and **b** juniper (anisohydric). Different colors denote different treatments where A stands for ambient, H for heat, D for drought, and H+D for heat and drought

Fig. 2 Calculated conductance (g) from Eq. 12 as a function of measured conductance from sap flux density FD for **a** piñon pine and **b** juniper. Different colors denote different treatments where A stands for ambient, H for heat, D for drought, and H+D for heat and drought

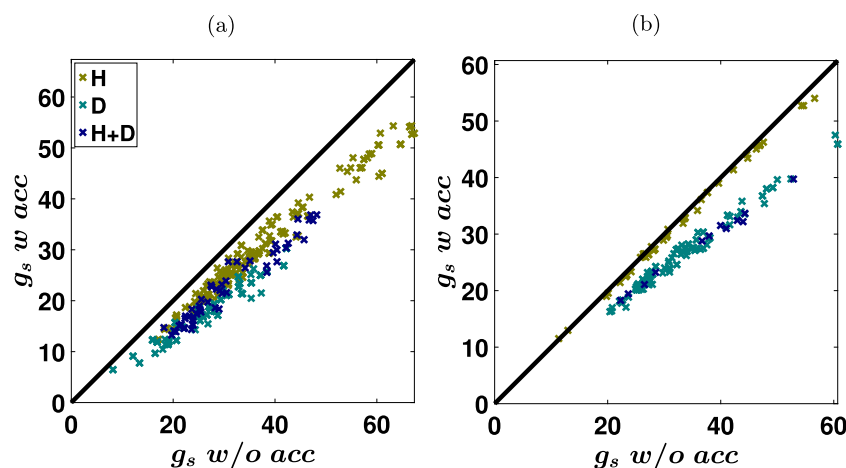


Water Effects

The effect of acclimation of hydraulic traits can be explored in a similar manner. As discussed earlier, the marginal water use efficiency λ represents the integrated effects of the water uptake strategies for the plant. In this case, studying the changes in λ and their effects on g for each treatment highlights the acclimation of hydraulic traits of a plant. To do so, g was calculated using the marginal water use efficiency of the ambient conditions, which is the fitted one and shown in Fig. 1, while accounting for the photosynthetic parameters of each treatment shown in Table 2. Figure 4 a and b show these results for piñon pine and juniper, respectively. In these figures, g with acclimation, which is the calculated g from the fitted parameters as discussed in “[Re-examining Recent Field Experiments](#)” section, is plotted against g without acclimation, which is the calculated g using λ for ambient conditions as discussed earlier, for different treatments.

Again, the deviation from the one-to-one line highlights the effect of hydraulic acclimation. As one can see from these figures, the behavior of each species was different as expected because of their isohydric and anisohydric stomatal behavior.

Fig. 3 Results highlighting the effects of photosynthetic parameters acclimation on stomatal conductance for **a** piñon pine and **b** juniper. Different colors denote different treatments where H stands for heat, D for drought, and H+D for heat and drought

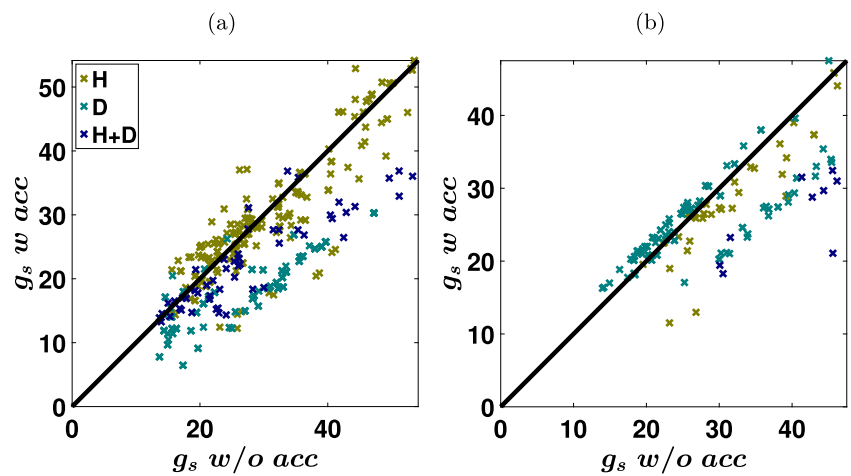


In Fig. 3a, piñon pine showed a decrease in stomatal conductance for all treatments with drought showing the highest impact, 30% with a 1% change for heated, and 15% for heat and drought. However, juniper showed a constant behavior for drought (around 4% decrease in conductance, and this is due to some points with extreme values) while decreasing the stomatal conductance for heated (around 11%) and heat and drought conditions (around 34%) as shown in Fig. 4b. This result highlights the anisohydric behavior of juniper that maintains its stomatal conductance much better during drought compared to piñon pine. Another difference is apparent in the heat and drought conditions where the heat offset the drought effects for piñon pine, which was not the case for juniper where the heat exacerbated the result. The Supplementary Table S4 shows the deviation statistics for all treatments and both species.

Cumulative Effects

The total effect of acclimation can also be shown so as to discuss the interactive effect of both physiological traits. To study these interactive effects, g was calculated using the

Fig. 4 Results highlighting the effects of hydraulic traits acclimation on stomatal conductance for **a** piñon pine and **b** juniper. Different colors denote different treatments where H stands for heat, D for drought, and H+D for heat and drought

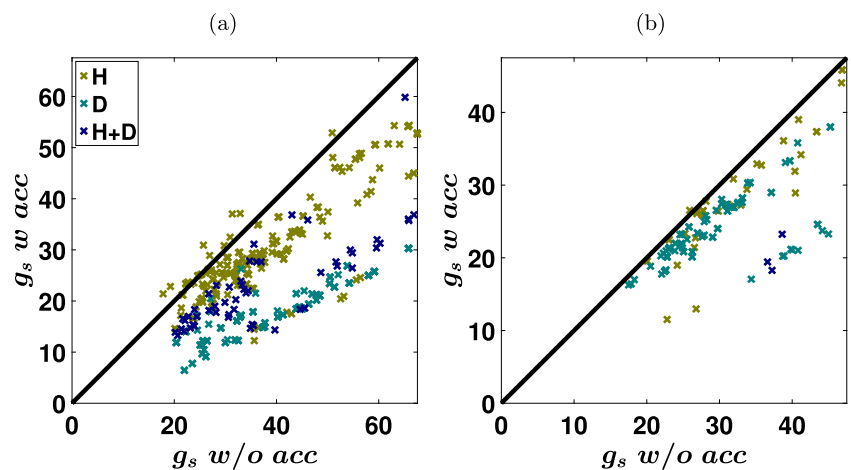


marginal water use efficiency and the photosynthetic parameters of the ambient conditions, which are shown in Fig. 1 and Table 2 respectively. Figures 5 a and b feature these results for piñon pine and juniper respectively. In these figures, the stomatal conductance with acclimation, which is the calculated g from the fitted parameters as discussed in “Re-examining Recent Field Experiments” section, is plotted against the stomatal conductance without acclimation, which is the calculated g using λ and V_{cmax} for ambient conditions as discussed earlier, for all treatments.

Again, the deviation from the one-to-one line highlights the effect of acclimation on both physiological traits. For all treatments, piñon pine appears less tolerant to a changing environment compared to juniper. This assertion stems from the fact that acclimation occurred in both species, yet the piñon pine did experience a decrease in the overall stomatal conductance despite acclimation in both hydraulic and physiological parameters. The highest impact was apparent in drought conditions as shown in Fig. 5a where the decrease in stomatal conductance was around 53%. Heated conditions exhibited the lowest reductions with stomatal conductance

decreasing by only 19%. For heat and drought, the result was less severe (around 37%) compared to drought-only as expected from “Water Effects” section. On the other hand, juniper was more resilient to drought where stomatal conductance decrease was around 23%. It was even better for heated conditions (around 13%) and more severe for heat and drought (around 48%) as shown in Fig. 5b. From these figures, one can see that the highest impact on g was due to hydraulic traits, and this is expected since plants are more affected by drought, which increases the cost for the plant to photosynthesize, compared to heating. The Supplementary Table S5 shows the deviation statistics for all treatments and both species. Overall, the insights into the controls of stomatal conductance responses to drought between isohydric piñon pine and anisohydric juniper match earlier experimental findings [37•]. Piñon pine reacts more to drought, and juniper reacts more to heating. Finally, the water potential at turgor loss has been used as a functional trait for determining plant drought tolerance. Species with a more negative turgor loss point have been shown to maintain significant g and carbon uptake under drier conditions [129].

Fig. 5 Results highlighting the effects of cumulative acclimation on stomatal conductance for **a** piñon pine and **b** Juniper. Different colors denote different treatments where H stands for heat, D for drought, and H+D for heat and drought



Interestingly, [130] showed that piñon pine does not perform osmoregulation in response to decreasing water status, while juniper turgor loss point fluctuates in concert with leaf water potential (from -3.4 to -6.6 MPa). Therefore, it is likely that the plastic response to drought of juniper trees was also possible because this species could control its turgor loss point compared to the isohydric piñon pine and thus adjust to drought and heated conditions to avoid tissue dehydration.

Conclusions

Models of photosynthesis are essential for understanding and predicting the functioning of terrestrial ecosystems, which account for about 56 and 30% of the global fluxes of carbon dioxide and water, respectively [131]. By understanding how stomatal kinetics function and drive photosynthesis, and how they are influenced by temperature and water availability, how plants respond to changes in their environment can then be conjectured. These conjectures can be used to assess the effects of extreme hydroclimatic conditions on ecosystem services.

The work here reviewed and showed how optimality principles can be employed to diagnose the effects of future changes in temperature and in soil water content and their impact on the water use efficiency and acclimation of tree species with contrasting stomatal behavior. This approach provides a scientific basis for understanding and predicting the impact of changing environmental conditions on forest functioning. The analyses describe what regulates the exchange of water vapor and carbon dioxide between the plant and the atmosphere under different environmental conditions assuming that stomata maximize carbon gain under soil water availability constraints. This optimality principle provides a reference state for stomatal kinetics that can then be contrasted to actual measurements. When measurements deviate from these predictions, these deviations suggest additional constraints (e.g., nutrients) or acclimation factors (e.g., $V_{c,max}$) to be significant. The optimality model developed here makes a number of assumptions (e.g., linear biochemical demand function, temporal changes in stomatal aperture are much faster than temporal changes in soil water availability) that can be relaxed albeit at the expense of mathematically more complex expressions or numerical models. Moreover, carry-over (or legacy) effects have not been treated explicitly though they can be via dynamic optimality theories (i.e., those that evolve λ in time and soil water). The effects of soil water stress on mesophyll conductance alone or the explicit inclusion of soil-plant hydraulic constraints can generate such legacy effects [132]. The persistence of drought effect can occur due to changes in leaf hydraulic conductance following vein cavitation-induced embolism and/or reduction in mesophyll hydraulic conductance that cannot

rapidly be repaired before rain resumes or new xylem tissue is added [15, 119, 133]. Other goal-seeking functions can also be selected to be maximized or minimized instead of L_o reflecting different strategies to describing stomatal aperture kinetics. In short, balancing biochemical demand to atmospheric supply of CO_2 yields an indeterminate problem necessitating at least one additional expression for stomatal conductance. Historically, this expression was provided empirically. Optimality theories offer a viable and attractive alternative to such closure as they encode generic statements presumed to be applicable to most terrestrial plants now and in a climatically altered future.

Supplementary Information The online version contains supplementary material available at <https://doi.org/10.1007/s40725-023-00202-4>.

Funding This work was supported by the US National Science Foundation (NSF-IOS-1754893, NSF-AGS-2028633), the Department of Energy (DE-SC0022072 and DE-SC0023309), the Los Alamos Directed Research and Development Exploratory Research Grant (No. 2020109DR), and the region Nlle. Aquitaine (projects VITIPIN, ANR PHydrauCC).

Data Availability The datasets generated for this study are available upon request to the corresponding author.

Declarations

Conflict of Interest The authors declare that they have no conflict of interest.

Human and Animal Rights and Informed Consent This article does not contain any studies with human or animal subjects performed by any of the authors.

References

Papers of particular interest, published recently, have been highlighted as:

- Of importance
- Of major importance

1. Liu H, Park Williams A, Allen CD, Guo D, Wu X, Anenkhonov OA, Liang E, Sandanov DV, Yin Y, Qi Z, et al. Rapid warming accelerates tree growth decline in semi-arid forests of inner Asia. *Glob Chang Biol*. 2013;19(8):2500–10.
2. Park WA, Allen CD, Macalady AK, Griffin D, Woodhouse CA, Meko DM, Swetnam TW, Rauscher SA, Seager R, Grissino-Mayer HD, et al. Temperature as a potent driver of regional forest drought stress and tree mortality. *Nat Clim Chang*. 2013;3(3):292–7.
3. Giannakopoulos C, Hadjinicolaou P, Kostopoulou E, Varotsos KV, Zerefos C. Precipitation and temperature regime over Cyprus as a result of global climate change. *Adv Geosci*. 2010;23:17–24. <https://doi.org/10.5194/adgeo-23-17-2010>.
4. Vogel MM, Orth R, Cheruy F, Hagemann S, Lorenz R, Hurk BJ, Seneviratne SI. Regional amplification of projected changes

- in extreme temperatures strongly controlled by soil moisture-temperature feedbacks. *Geophys Res Lett*. 2017;44(3):1511–9.
5. Givnish TJ. Comparative studies of leaf form: assessing the relative roles of selective pressures and phylogenetic constraints. *New Phytol*. 1987;106:131–60.
 6. Pittermann J, Stuart SA, Dawson TE, Moreau A. Cenozoic climate change shaped the evolutionary ecophysiology of the Cupressaceae conifers. *Proc Natl Acad Sci*. 2012;109(24):9647–52.
 7. Johnson HB. Plant pubescence: an ecological perspective. *Bot Rev*. 1975;41:233–58.
 8. Hacke UG, Spicer R, Schreiber SG, Plavcová L. An ecophysiological and developmental perspective on variation in vessel diameter. *Plant Cell Environ*. 2017;40(6):831–45.
 9. Olson ME, Anfodillo T, Gleason SM, McCulloh KA. Tip-to-base xylem conduit widening as an adaptation: causes, consequences, and empirical priorities. *New Phytol*. 2021;229(4):1877–93.
 10. Rodríguez-Ramírez EC, Ferrero ME, Acevedo-Vega I, Crispin-DelaCruz DB, Ticse-Otarola G, Requena-Rojas EJ. Plastic adjustments in xylem vessel traits to drought events in three *Cedrela* species from Peruvian Tropical Andean forests. *Scientific Reports*. 2022;12(1):21112.
 11. Martin RE, Asner GP, Bentley LP, Shenkin A, Salinas N, Huaypar KQ, Pillco MM, Ccori Álvarez FD, Enquist BJ, Diaz S, et al. Covariance of sun and shade leaf traits along a tropical forest elevation gradient. *Front Plant Sci*. 2020;10:1810.
 12. Givnish TJ. Adaptation to sun and shade: a whole-plant perspective. *Funct Plant Biol*. 1988;15(2):63–92.
 13. Tardieu F, Simonneau T. Variability among species of stomatal control under fluctuating soil water status and evaporative demand: modelling isohydric and anisohydric behaviours. *J Exp Bot*. 1998;419–432.
 14. Stocker O. Die abhängigigkeit der transpiration von den umweltfaktoren. 1956;436–488.
 15. Domec J-C, Johnson DM. Does homeostasis or disturbance of homeostasis in minimum leaf water potential explain the isohydric versus anisohydric behavior of *Vitis vinifera* L. cultivars? *Tree Physiol*. 2012;32(3):245–248.
 16. Meinzer FC, Woodruff DR, Marias DE, Smith DD, McCulloh KA, Howard AR, Magedman AL. Mapping ‘hydroscares’ along the iso-to anisohydric continuum of stomatal regulation of plant water status. *Ecol Lett*. 2016;19(11):1343–52.
 - 17.● Martínez-Vilalta J, Garcia-Forner N. Water potential regulation, stomatal behaviour and hydraulic transport under drought: deconstructing the iso/anisohydric concept. *Plant Cell Environ*. 2017;40(6):962–976. **This review explains the difference between isohydric and anisohydric behavior and shows the existence of a continuum for this behavior.**
 18. Adams HD, Zeppel MJ, Anderegg WR, Hartmann H, Landhäusser SM, Tissue DT, Huxman TE, Hudson PJ, Franz TE, Allen CD, et al. A multi-species synthesis of physiological mechanisms in drought-induced tree mortality. *Nature Ecol Evol*. 2017;1(9):1285–91.
 19. Parolari AJ, Katul GG, Porporato A. An ecohydrological perspective on drought-induced forest mortality. *J Geophys Res Biogeosci*. 2014;119(5):965–81.
 20. Attia Z, Domec J-C, Oren R, Way DA, Moshelion M. Growth and physiological responses of isohydric and anisohydric poplars to drought. *J Exp Bot*. 2015;66(14):4373–81.
 21. Yi K, Maxwell JT, Wenzel MK, Roman DT, Sauer PE, Phillips RP, Novick KA. Linking variation in intrinsic water-use efficiency to isohydricity: a comparison at multiple spatiotemporal scales. *New Phytol*. 2019;221(1):195–208.
 22. Plaut JA, Yezpe EA, Hill J, Pangle R, Sperry JS, Pockman WT, McDowell NG. Hydraulic limits preceding mortality in a piñon-juniper woodland under experimental drought. *Plant Cell Environ*. 2012;35(9):1601–17.
 23. Limousin J-M, Bickford CP, Dickman LT, Pangle RE, Hudson PJ, Boutz AL, Gehres N, Osuna JL, Pockman WT, McDowell NG. Regulation and acclimation of leaf gas exchange in a piñon-juniper woodland exposed to three different precipitation regimes. *Plant Cell Environ*. 2013;36(10):1812–25.
 24. McDowell NG, Fisher RA, Xu C, Domec J-C, Hölttä T, Mackay DS, Sperry JS, Boutz A, Dickman L, Gehres N, et al. Evaluating theories of drought-induced vegetation mortality using a multimodel-experiment framework. *New Phytol*. 2013;200(2):304–21.
 25. McDowell N, Pockman WT, Allen CD, Breshears DD, Cobb N, Kolb T, Plaut J, Sperry J, West A, Williams DG, et al. Mechanisms of plant survival and mortality during drought: why do some plants survive while others succumb to drought? *New Phytol*. 2008;178(4):719–39.
 26. Hoffmann WA, Marchin RM, Abit P, Lau OL. Hydraulic failure and tree dieback are associated with high wood density in a temperate forest under extreme drought. *Glob Chang Biol*. 2011;17(8):2731–42.
 27. Garcia-Forner N, Adams HD, Sevanto S, Collins AD, Dickman LT, Hudson PJ, Zeppel MJ, Jenkins MW, Powers H, Martínez-Vilalta J, et al. Responses of two semiarid conifer tree species to reduced precipitation and warming reveal new perspectives for stomatal regulation. *Plant Cell Environ*. 2016;39(1):38–49.
 28. Pappas C, Matheny AM, Baltzer JL, Barr AG, Black TA, Bohrer G, Detto M, Maillet J, Roy A, Sonnentag O, et al. Boreal tree hydrodynamics: asynchronous, diverging, yet complementary. *Tree Physiol*. 2018;38(7):953–64.
 29. Fisher RA, Williams M, Do Vale RL, Da Costa AL, Meir P. Evidence from Amazonian forests is consistent with isohydric control of leaf water potential. *Plant Cell Environ*. 2006;29(2):151–65.
 30. Klein T. The variability of stomatal sensitivity to leaf water potential across tree species indicates a continuum between isohydric and anisohydric behaviours. *Funct Ecol*. 2014;28(6):1313–20.
 31. Benson MC, Minit CF, Oishi AC, Denham SO, Domec J-C, Johnson DM, Missik JE, Phillips RP, Wood JD, Novick KA. The xylem of anisohydric *Quercus alba* L. is more vulnerable to embolism than isohydric codominants. *Plant Cell Environ*. 2022;45(2):329–346.
 32. Collins MJ, Fuentes S, Barlow EW. Partial rootzone drying and deficit irrigation increase stomatal sensitivity to vapour pressure deficit in anisohydric grapevines. *Funct Plant Biol*. 2010;37(2):128–38.
 33. Romero-Trigueros C, Gambín JMB, Nortes Tortosa PA, Cabañero JJA, Nicolás EN. Isohydricity of two different citrus species under deficit irrigation and reclaimed water conditions. *Plants*. 2021;10(10):2121.
 34. Schultz HR. Differences in hydraulic architecture account for near-isohydric and anisohydric behaviour of two field-grown *Vitis vinifera* L. cultivars during drought. *Plant Cell Environ*. 2003;26(8):1393–1405.
 35. Johnson DM, Katul G, Domec J-C. Catastrophic hydraulic failure and tipping points in plants. *Plant Cell Environ*. 2022.
 36. Zeppel MJ, Lewis JD, Chaszar B, Smith RA, Medlyn BE, Huxman TE, Tissue DT. Nocturnal stomatal conductance responses to rising [CO₂], temperature and drought. *New Phytol*. 2012;193(4):929–38.
 - 37.● Grossiord C, Sevanto S, Borrego I, Chan AM, Collins AD, Dickman LT, Hudson PJ, McBranch N, Michaletz ST, Pockman WT, et al. Tree water dynamics in a drying and warming world. *Plant Cell Environ*. 2017;40(9):1861–1873. **This article provides a**

- detailed explanation for the experiment and data used to generate the results of the case study.**
38. Givnish TJ, Vermeij GJ. Sizes and shapes of liane leaves. *Am Nat.* 1976;110(975):743–78.
 39. Mäkelä A, Berninger F, Hari P. Optimal control of gas exchange during drought: theoretical analysis. *Ann Bot.* 1996;77(5):461–8.
 - 40.●● Cowan I, Troughton J. The relative role of stomata in transpiration and assimilation. *Planta.* 1971;97(4):325–336. **This manuscript introduces the formulation of stomatal optimality principle in plant physiology necessary for the development of the approach used in this study.**
 41. Papert S. Mindstorms: computers, children, and powerful ideas. 1980;230.
 42. Bardi U. Mind sized world models. *Sustainability.* 2013;5(3):896–911.
 43. Franklin O, Harrison SP, Dewar R, Farrow CE, Brännström Å, Dieckmann U, Pietsch S, Falster D, Cramer W, Loreau M, et al. Organizing principles for vegetation dynamics. *Nature Plants.* 2020;6(5):444–53.
 44. Ainsworth EA, Rogers A. The response of photosynthesis and stomatal conductance to rising [CO₂]: mechanisms and environmental interactions. *Plant Cell Environ.* 2007;30(3):258–70.
 45. Buckley TN. The control of stomata by water balance. *New Phytol.* 2005;168(2):275–92.
 46. Campbell GS, Norman JM. An introduction to environmental biophysics. 2000.
 - 47.● Damour G, Simonneau T, Cochard H, Urban L. An overview of models of stomatal conductance at the leaf level. *Plant Cell Environ.* 2010;33(9):1419–1438. **This article provides an overview of the different stomatal conductance models.**
 48. Farquhar GD, Sharkey TD. Stomatal conductance and photosynthesis. *Annu Rev Plant Physiol.* 1982;33(1):317–45.
 - 49.● Hetherington AM, Woodward FI. The role of stomata in sensing and driving environmental change. *Nature.* 2003;424(6951):901–908. **This paper highlights the role of stomata and intercellular CO₂ in regulating climate models.**
 50. Hallé F, Jones HG—Plants and microclimate. A quantitative approach to environmental plant physiology. Cambridge university press, Cambridge, 1983. *Revue d'Écologie (La Terre et La Vie).* 1984;39(1):123–123.
 51. Meidner H, Zeiger E, Farquhar G, Cowan I. Three hundred years of research into stomata. *Stomatal Function.* 1987;7–27.
 52. Schulze E-D, Kelliher FM, Körner C, Lloyd J, Leuning R. Relationships among maximum stomatal conductance, ecosystem surface conductance, carbon assimilation rate, and plant nitrogen nutrition: a global ecology scaling exercise. *Annu Rev Ecol Syst.* 1994;25(1):629–62.
 53. Darwin F. IX. Observations on stomata. *Philos Trans R Soc Lond B Containing Papers Biol Char.* 1898;190:531–621.
 54. Scarth GW. Stomatal movement: its regulation and regulatory role a review. *Protoplasma.* 1927;2(1):498–511.
 55. Bowen IS. The ratio of heat losses by conduction and by evaporation from any water surface. *Phys Rev.* 1926;27(6):779.
 56. Penman HL. Natural evaporation from open water, bare soil and grass. *Proc R Soc Lond A Math Phys Sci.* 1948;193(1032):120–45.
 57. Monteith JL. Evaporation and environment. In: *Symposia of the Society for Experimental Biology.* Cambridge: University Press (CUP) Cambridge; 1965. vol. 19, p. 205–234.
 58. Jarvis P. The interpretation of the variations in leaf water potential and stomatal conductance found in canopies in the field. *Philos Trans R Soc Lond B Biol Sci.* 1976;273(927):593–610.
 59. Collatz GJ, Ball JT, Grivet C, Berry JA. Physiological and environmental regulation of stomatal conductance, photosynthesis and transpiration: a model that includes a laminar boundary layer. *Agric Forest Meteorol.* 1991;54(2):107–36. [https://doi.org/10.1016/0168-1923\(91\)90002-8](https://doi.org/10.1016/0168-1923(91)90002-8).
 60. Leuning R. A critical appraisal of a combined stomatal-photosynthesis model for C3 plants. *Plant Cell Environ.* 1995;18(4):339–55.
 61. Ball JT, Woodrow IE, Berry JA. A model predicting stomatal conductance and its contribution to the control of photosynthesis under different environmental conditions. In: *Progress in Photosynthesis Research: Volume 4 Proceedings of the VIIIth International Congress on Photosynthesis* Providence, Rhode Island, USA, August 10–15, 1986. Springer 1987. p. 221–224.
 62. Sellers P, Bounoua L, Collatz G, Randall D, Dazlich D, Los S, Berry J, Fung I, Tucker C, Field C, et al. Comparison of radiative and physiological effects of doubled atmospheric CO₂ on climate. *Science.* 1996;271(5254):1402–6.
 - 63.● Oren R, Sperry J, Katul G, Pataki D, Ewers B, Phillips N, Schäfer K. Survey and synthesis of intra- and interspecific variation in stomatal sensitivity to vapour pressure deficit. *Plant Cell Environ.* 1999;22(12):1515–1526. **This work demonstrates the universal role of stomata in response to vapor pressure deficit from different set of data.**
 64. Sperry J, Hacke U, Oren R, Comstock J. Water deficits and hydraulic limits to leaf water supply. *Plant Cell Environ.* 2002;25(2):251–63.
 65. Liu Y, Kumar M, Katul GG, Feng X, Konings AG. Plant hydraulics accentuate the effect of atmospheric moisture stress on transpiration. *Nat Clim Chang.* 2020;10(7):691–5.
 66. Cowan I. Stomatal behaviour and environment. In: *Advances in Botanical Research.* Elsevier, ??? 1978. vol. 4, p. 117–228
 67. Cowan IR, GD F. Stomatal function in relation to leaf metabolism and environment. 1977.
 68. Hari P, Mäkelä A, Korpilahti E, Holmberg M. Optimal control of gas exchange. *Tree Physiol.* 1986;2(1-2-3):169–175.
 69. Berninger F, Hari P. Optimal regulation of gas exchange: evidence from field data. *Ann Bot.* 1993;71(2):135–40.
 70. Hari P, Mäkelä A, Pohja T. Surprising implications of the optimality hypothesis of stomatal regulation gain support in a field test. *Funct Plant Biol.* 2000;27(1):77–80.
 71. Arneth A, Lloyd J, Santrckova H, Bird M, Grigoryev S, Kalaschnikov Y, Gleixner G, Schulze E-D. Response of central Siberian scots pine to soil water deficit and long-term trends in atmospheric CO₂ concentration. *Glob Biogeochem Cycles.* 2002;16(1):5–1.
 72. Konrad W, Roth-Nebelsick A, Grein M. Modelling of stomatal density response to atmospheric CO₂. *J Theor Biol.* 2008;253(4):638–58.
 73. Katul GG, Palmroth S, Oren R. Leaf stomatal responses to vapour pressure deficit under current and CO₂-enriched atmosphere explained by the economics of gas exchange. *Plant Cell Environ.* 2009;32(8):968–79.
 74. Medlyn BE, Duursma RA, Eamus D, Ellsworth DS, Prentice IC, Barton CV, Crous KY, De Angelis P, Freeman M, Wingate L. Reconciling the optimal and empirical approaches to modelling stomatal conductance. *Glob Chang Biol.* 2011;17(6):2134–2144.
 75. Katul G, Manzoni S, Palmroth S, Oren R. A stomatal optimization theory to describe the effects of atmospheric CO₂ on leaf photosynthesis and transpiration. *Ann Bot.* 2010;105(3):431–42.
 76. Katul GG, Oren R, Manzoni S, Higgins C, Parlange MB. Evapotranspiration: a process driving mass transport and energy exchange in the soil-plant-atmosphere-climate system. *Rev Geophys.* 2012;50(3).

77. Tuzet A, Perrier A, Leuning R. A coupled model of stomatal conductance, photosynthesis and transpiration. *Plant Cell Environ.* 2003;26(7):1097–116.
78. Lai C-T, Katul G, Oren R, Ellsworth D, Schäfer K. Modeling CO₂ and water vapor turbulent flux distributions within a forest canopy. *J Geophys Res Atmos.* 2000;105(D21):26333–51.
79. Cowan I, et al. Economics of carbon fixation in higher plants. *Economics of carbon fixation in higher plants.* 1986. p. 133–170.
80. Manzoni S, Vico G, Palmroth S, Porporato A, Katul G. Optimization of stomatal conductance for maximum carbon gain under dynamic soil moisture. *Adv Water Resour.* 2013;62:90–105.
- 81.●● Mrad A, Sevanto S, Domec J-C, Liu Y, Nakad M, Katul G. A dynamic optimality principle for water use strategies explains isohydric to anisohydric plant responses to drought. *Front Forest Global Change.* 2019;2:49. **This study provides a derivation for the dynamic optimality principles and shows the connections between the Hamiltonian and physiological fluxes.**
82. Feng X, Lu Y, Jiang M, Katul G, Manzoni S, Mrad A, Vico G. Instantaneous stomatal optimization results in suboptimal carbon gain due to legacy effects. *Plant Cell Environ.* 2022
83. Manzoni S, Vico G, Katul G, Fay PA, Polley W, Palmroth S, Porporato A. Optimizing stomatal conductance for maximum carbon gain under water stress: a meta-analysis across plant functional types and climates. *Funct Ecol.* 2011;25(3):456–67.
84. Parlange J-Y, Waggoner PE. Stomatal dimensions and resistance to diffusion. *Plant Physiol.* 1970;46(2):337–42.
85. Witelski T, Bowen M. Variational Principles. In: Witelski T, Bowen M, editors. *Methods of mathematical modelling: continuous systems and differential equations.* Springer Undergraduate Mathematics Series. Springer: Cham; 2015. p. 47–83. https://doi.org/10.1007/978-3-319-23042-9_3.
86. Fites J, Teskey R. CO₂ and water vapor exchange of *Pinus taeda* in relation to stomatal behavior: test of an optimization hypothesis. *Can J For Res.* 1988;18(2):150–7.
- 87.●● Farquhar GD, Caemmerer Sv, Berry JA. A biochemical model of photosynthetic CO₂ assimilation in leaves of C₃ species. *Planta.* 1980;149(1):78–90. **This study covers the formulation of the biochemical demand for CO₂ by C₃ plants, a necessary step for the conceptualization of stomatal optimization.**
88. Qiu R, Katul GG. Maximizing leaf carbon gain in varying saline conditions: an optimization model with dynamic mesophyll conductance. *Plant J.* 2020;101(3):543–54.
89. Volpe V, Manzoni S, Marani M, Katul G. Leaf conductance and carbon gain under salt-stressed conditions. *J Geophys Res Biogeosci.* 2011;116(G4).
90. Mackay D, Ahl D, Ewers B, Samanta S, Gower S, Burrows S. Physiological tradeoffs in the parameterization of a model of canopy transpiration. *Adv Water Resour.* 2003;26(2):179–94.
91. Launiainen S, Katul GG, Kolari P, Vesala T, Hari P. Empirical and optimal stomatal controls on leaf and ecosystem level CO₂ and H₂O exchange rates. *Agric Forest Meteorol.* 2011;151(12):1672–89.
- 92.● Monteith J. A reinterpretation of stomatal responses to humidity. *Plant Cell Environ.* 1995;18(4):357–364. **This manuscript introduces the feed-forward mechanism of stomata. This mechanism is apparent in the result of stomatal optimization.**
93. Schulze E-D, Lange O, Buschbom U, Kappen L, Evenari M. Stomatal responses to changes in humidity in plants growing in the desert. *Planta.* 1972;108(3):259–70.
94. Franks P, Cowan I, Farquhar G. The apparent feedforward response of stomata to air vapour pressure deficit: information revealed by different experimental procedures with two rainforest trees. *Plant Cell Environ.* 1997;20(1):142–5.
95. Lhomme J-P. Stomatal control of transpiration: examination of the Jarvis-type representation of canopy resistance in relation to humidity. *Water Resour Res.* 2001;37(3):689–99.
96. Turner NC, Schulze E-D, Gollan T. The responses of stomata and leaf gas exchange to vapour pressure deficits and soil water content. *Oecologia.* 1984;63(3):338–42.
97. Macfarlane C, White D, Adams M. The apparent feed-forward response to vapour pressure deficit of stomata in droughted, field-grown *Eucalyptus globulus* Labill. *Plant Cell Environ.* 2004;27(10):1268–80.
98. Duursma RA, Barton CV, Lin Y-S, Medlyn BE, Eamus D, Tissue DT, Ellsworth DS, McMurtrie RE. The peaked response of transpiration rate to vapour pressure deficit in field conditions can be explained by the temperature optimum of photosynthesis. *Agric Forest Meteorol.* 2014;189:2–10.
99. Vico G, Manzoni S, Palmroth S, Weih M, Katul G. A perspective on optimal leaf stomatal conductance under CO₂ and light limitations. *Agric Forest Meteorol.* 2013;182:191–9.
100. Palmroth S, Berninger F, Nikinmaa E, Lloyd J, Pulkkinen P, Hari P. Structural adaptation rather than water conservation was observed in Scots pine over a range of wet to dry climates. *Oecologia.* 1999;121(3):302–9.
101. Wong S, Dunin F. Photosynthesis and transpiration of trees in a eucalypt forest stand: CO₂, light and humidity responses. *Funct Plant Biol.* 1987;14(6):619–32.
102. Katul G, Ellsworth D, Lai C-T. Modelling assimilation and intercellular CO₂ from measured conductance: a synthesis of approaches. *Plant Cell Environ.* 2000;23(12):1313–28.
103. Zhou S, Yu B, Huang Y, Wang G. Daily underlying water use efficiency for AmeriFlux sites. *J Geophys Res Biogeosci.* 2015;120(5):887–902.
104. Nelson JA, Pérez-Priego O, Zhou S, Poyatos R, Zhang Y, Blanken PD, Gimeno TE, Wohlfahrt G, Desai AR, Gioli B, et al. Ecosystem transpiration and evaporation: insights from three water flux partitioning methods across FLUXNET sites. *Glob Chang Biol.* 2020;26(12):6916–30.
105. Zhou S, Yu B, Zhang Y, Huang Y, Wang G. Partitioning evapotranspiration based on the concept of underlying water use efficiency. *Water Resour Res.* 2016;52(2):1160–75.
106. Perez-Priego O, Katul G, Reichstein M, El-Madany TS, Ahrens B, Carrara A, Scanlon TM, Migliavacca M. Partitioning eddy covariance water flux components using physiological and micrometeorological approaches. *J Geophys Res Biogeosci.* 2018;123(10):3353–70.
107. Zahn E, Bou-Zeid E, Good SP, Katul GG, Thomas CK, Ghannam K, Smith JA, Chamecki M, Dias NL, Fuentes JD, et al. Direct partitioning of eddy-covariance water and carbon dioxide fluxes into ground and plant components. *Agric Forest Meteorol.* 2022;315: 108790.
108. Mott K, Parkhurst D. Stomatal responses to humidity in air and Helox. *Plant Cell Environ.* 1991;14(5):509–15.
109. Siqueira M, Katul G, Porporato A. Onset of water stress, hysteresis in plant conductance, and hydraulic lift: scaling soil water dynamics from millimeters to meters. *Water Resour Res.* 2008;44(1).
110. Siqueira M, Katul G, Porporato A. Soil moisture feedbacks on convection triggers: the role of soil-plant hydrodynamics. *J Hydrometeorol.* 2009;10(1):96–112.
111. Manoli G, Bonetti S, Domec J-C, Putti M, Katul G, Marani M. Tree root systems competing for soil moisture in a 3D soil-plant model. *Adv Water Resour.* 2014;66:32–42.
112. Manoli G, Huang C-W, Bonetti S, Domec J-C, Marani M, Katul G. Competition for light and water in a coupled soil-plant system. *Adv Water Resour.* 2017;108:216–30.

113. Sperry JS, Love DM. What plant hydraulics can tell us about responses to climate-change droughts. *New Phytol.* 2015;207(1):14–27.
114. Huang CW, Domec JC, Palmroth S, Pockman WT, Litvak ME, Katul GG. Transport in a coordinated soil-root-xylem-phloem leaf system. *Adv Water Resour.* 2018;119:1–16.
115. Sperry JS, Venturas MD, Anderegg WR, Mencuccini M, Mackay DS, Wang Y, Love DM. Predicting stomatal responses to the environment from the optimization of photosynthetic gain and hydraulic cost. *Plant Cell Environ.* 2017;40(6):816–30.
116. Anderegg WR, Wolf A, Arango-Velez A, Choat B, Chmura DJ, Jansen S, Kolb T, Li S, Meinzer FC, Pita P, et al. Woody plants optimise stomatal behaviour relative to hydraulic risk. *Ecol Lett.* 2018;21(7):968–77.
117. Venturas MD, Sperry JS, Hacke UG. Plant xylem hydraulics: what we understand, current research, and future challenges. *J Integr Plant Biol.* 2017;59(6):356–89.
118. Dewar R, Maurantan A, Mäkelä A, Hölttä T, Medlyn B, Vesala T. New insights into the covariation of stomatal, mesophyll and hydraulic conductances from optimization models incorporating nonstomatal limitations to photosynthesis. *New Phytol.* 2018;217(2):571–85.
119. Flexas J, Scoffoni C, Gago J, Sack L. Leaf mesophyll conductance and leaf hydraulic conductance: an introduction to their measurement and coordination. *J Exp Bot.* 2013;64(13):3965–81.
120. Jensen KH, Lee J, Bohr T, Bruus H, Holbrook NM, Zwieniecki MA. Optimality of the Münch mechanism for translocation of sugars in plants. *J R Soc Interface.* 2011;8(61):1155–65.
121. Nikinmaa E, Hölttä T, Hari P, Kolari P, Mäkelä A, Sevanto S, Vesala T. Assimilate transport in phloem sets conditions for leaf gas exchange. *Plant Cell Environ.* 2013;36(3):655–69.
122. Nikinmaa E, Sievänen R, Hölttä T. Dynamics of leaf gas exchange, xylem and phloem transport, water potential and carbohydrate concentration in a realistic 3-D model tree crown. *Ann Bot.* 2014;114(4):653–66.
123. Nakad M, Domec J-C, Sevanto S, Katul G. Radial-axial transport coordination enhances sugar translocation in the phloem vasculature of plants. *Plant Physiol.* 2022. <https://doi.org/10.1093/plphys/kiac231>.
124. Konrad W, Katul G, Roth-Nebelsick A, Jensen KH. Xylem functioning, dysfunction and repair: a physical perspective and implications for phloem transport. *Tree Physiol.* 2018;39(2):243–61.
125. Jensen KH, Berg-Sørensen K, Bruus H, Holbrook NM, Liesche J, Schulz A, Zwieniecki MA, Bohr T. Sap flow and sugar transport in plants. *Rev Mod Phys.* 2016;88(3):035007.
126. Prentice IC, Dong N, Gleason SM, Maire V, Wright IJ. Balancing the costs of carbon gain and water transport: testing a new theoretical framework for plant functional ecology. *Ecol Lett.* 2014;17(1):82–91.
127. Perri S, Katul GG, Molini A. Xylem-phloem hydraulic coupling explains multiple osmoregulatory responses to salt stress. *New Phytol.* 2019;224(2):644–62.
128. Katul G, Leuning R, Oren R. Relationship between plant hydraulic and biochemical properties derived from a steady-state coupled water and carbon transport model. *Plant Cell Environ.* 2003;26(3):339–50.
129. Turner NC. Turgor maintenance by osmotic adjustment: a review and evaluation. *Adaptation of plants to water and high temperature stress.* 1980. p. 87–103.
130. Meinzer FC, Woodruff DR, Marias DE, McCulloh KA, Sevanto S. Dynamics of leaf water relations components in co-occurring iso- and anisohydric conifer species. *Plant Cell Environ.* 2014;37(11):2577–86.
131. Jasechko S, Sharp ZD, Gibson JJ, Birks SJ, Yi Y, Fawcett PJ. Terrestrial water fluxes dominated by transpiration. *Nature.* 2013;496(7445):347–50.
132. Griffiths H, Helliwell BR. Mesophyll conductance: internal insights of leaf carbon exchange. *Plant Cell Environ.* 2013;36(4):733–5.
133. Brodersen CR, McElrone AJ. Maintenance of xylem network transport capacity: a review of embolism repair in vascular plants. *Front Plant Sci.* 2013;4:108.

Publisher's Note Springer Nature remains neutral with regard to jurisdictional claims in published maps and institutional affiliations.

Springer Nature or its licensor (e.g. a society or other partner) holds exclusive rights to this article under a publishing agreement with the author(s) or other rightsholder(s); author self-archiving of the accepted manuscript version of this article is solely governed by the terms of such publishing agreement and applicable law.

Authors and Affiliations

Mazen Nakad¹ · Sanna Sevanto² · Jean-Christophe Domec^{3,4} · Gabriel Katul^{1,4}

Sanna Sevanto
sanna@lanl.gov

Jean-Christophe Domec
jc.domec@duke.edu

Gabriel Katul
gaby@duke.edu

¹ Department of Civil and Environmental Engineering, Duke University, 404 Research Drive, Durham, NC 27708, USA

² Earth and Environmental Sciences Division, Los Alamos National Laboratory, Los Alamos, NM 87545, USA

³ UMR 1391 INRA-ISPRA, Bordeaux Sciences Agro, Gradignan, France

⁴ Nicholas School of the Environment, Duke University, Durham, NC 27708, USA